Biomolecular Adsorption Phenomena in Electrowetting-Based Digital Microfluidic Devices

A. Ahmadi*, K. D. Devlin*, H. Najjaran*, J. F. Holzman* and M. Hoorfar*

* University of British Columbia, Kelowna, BC, Canada, mina.hoorfar@ubc.ca

ABSTRACT

In this paper, the protein adsorption process in electrowetting-based digital microfluidic devices is investigated and modeled. An analytical method is used to develop a new formulation for the relationship between the time-varying contact angle and the applied voltage. It is found that the contact angle is a strong function of the protein bulk concentration as well as the protein molecular characteristics. The model describes the kinetics of the diffusion-controlled interfacial changes as well as the conformational changes of the adsorbed molecules. The accuracy of the model is verified by a direct comparison of these findings with experimental results. The comparison of the experimental and modeling results shows that the presented model is able to describe accurately the underlying physics of the biomolecular adsorption process, and insight is gained into the complexities of protein-based biochips.
Keywords: digital microfluidic, electrowetting, biomolecular adsorption

1 INTRODUCTION

Digital microfluidic lab-on-a-chip technology [1-3] has been a new trend in miniaturizing biomedical platforms [4]. In addition to reduced sample and reagent consumption, these devices offer higher levels of throughput and automation [5]. Recently, this technology has been employed in the development of integrated proteomics analysis methodologies [4, 6, 7]. In essence, the proteomics analysis is based on surface protein adsorption. However, nonspecific adsorption of these biomolecules has proven to be one of the greatest sources of uncertainties for these biofluidic chips [8]. Unwanted adsorption ultimately decreases the device sensitivity and severely limits the device performance [8]. An accurate understanding of the adsorption process on these biochips is needed to allow for successful device design and its implementation.

In this paper, the protein adsorption process in electrowetting-based digital microfluidic devices is investigated and modeled. The change in the interfacial tensions over time is modeled, and it is related to the change in the contact angle of the microdroplet and the system capacitance. In order to verify the developed model, capacitance of a digital microfluidic system is calculated as a function of time, and it is compared to the measured values. Finally, the model is used to predict the behavior of the system for two different biomolecules: BSA and lysozyme. It is shown that since BSA and lysozyme molecules have different charges, the contact angle and capacitance changes over time present different trends. Moreover, it is shown that polarity of the applied voltage plays a crucial role in the adsorption process.

2 THEORY

In this section an accurate formulation is derived to model protein adsorption in digital microfluidic systems. This model is capable of predicting the microdroplet and system behavior for different solutions.

Young's equation relates the interfacial tensions and the contact angle of the microdroplet as [9]

$$\gamma_{\mathrm{lv}} \cos\theta = \gamma_{\mathrm{sv}} - \gamma_{\mathrm{sl}}\,, \tag{1}$$

where γ_{sl}, γ_{lv} and γ_{sv} are the solid-liquid, liquid-vapor and solid-vapor interfacial tensions and θ is the contact angle of the microdroplet. Lippmann law, on the other hand, relates the change in the solid-liquid interfacial tension to the voltage difference across the underlying dielectric (and hydrophobic) layers as

$$\gamma_{\mathrm{sl},1} - \gamma_{\mathrm{sl},2} = \frac{cV^2}{2}\,, \tag{2}$$

where $\gamma_{\mathrm{sl},1}$ and $\gamma_{\mathrm{sl},2}$ are the solid-liquid interfacial tensions before and after applying voltage, V is the voltage difference across the underlying dielectric (and hydrophobic) layers. The capacitance c of the underlying layer per unit area is defined as

$$c = \frac{\varepsilon_0}{\sum_i d_i/\varepsilon_i}\,, \tag{3}$$

where d_i and ε_i are the thickness and dielectric constant of the ith layer, and ε_0 is the permittivity of free-space.

It has been shown that physical properties of the microdroplet interface, particularly the interfacial tensions, change due to the adsorption of the proteins at the interfaces. The change in the interfacial tensions is modeled as [10]

$$\gamma_{sl}(t)=\gamma_{sl}(\infty)+\left[\alpha_{sl}\exp\left(-\sqrt{\frac{4t}{\pi\tau_{sl}}}\right)+\beta_{sl}\right]\exp(-k_{sl}t) \quad (4)$$

and

$$\gamma_{lv}(t)=\gamma_{lv}(\infty)+\left[\alpha_{lv}\exp\left(-\sqrt{\frac{4t}{\pi\tau_{lv}}}\right)+\beta_{lv}\right]\exp(-k_{lv}t), \quad (5)$$

where $\gamma_{sl}(\infty)$ and $\gamma_{lv}(\infty)$ are the solid-liquid and liquid-vapor interfacial tensions in the steady state, τ_{sl} and τ_{lv} are diffusion relaxation times, t is the time, and k_{sl} and k_{lv} are the rate constants for the conformational changes at the interface. The total decreases in the interfacial tesnsions, $\gamma_{sl}(0)-\gamma_{sl}(\infty)$ and $\gamma_{lv}(0)-\gamma_{lv}(\infty)$, are composed of two parts: the diffusion-controlled adsorption part, α_{sl} and α_{lv}, and conformational changes of the adsorbed protein part, β_{sl} and β_{lv}.

Considering the effects of adsorption, Lippmann law can be modified as

$$\gamma_{sl0}-\gamma_{sl}(V,t)=\frac{c(t)V^2}{2}+\Delta\gamma_{sl,ads}, \quad (6)$$

where γ_{sl0} is the solid-liquid interfacial tension at time zero with zero applied voltage, and $\Delta\gamma_{sl,ads}$ is the change in the solid-liquid interfacial tension due to the adsorption phenomenon. Using equation (4), $\Delta\gamma_{sl,ads}$ can be written as

$$\Delta\gamma_{sl,ads}=\alpha_{sl}+\beta_{sl}-\left[\alpha_{sl}\exp\left(-\sqrt{\frac{4t}{\pi\tau_{sl}}}\right)+\beta_{sl}\right]\exp(-k_{sl}t). \quad (7)$$

On the other hand, Young's equation relates the solid-liquid interfacial tension. By combining the equations (1) and (6) the modified Lippmann law can be written as

$$-\gamma_{lv0}\cos\theta_0+\gamma_{lv}(t)\cos\theta(V,t)=\frac{c(t)V^2}{2}+\Delta\gamma_{sl,ads}, \quad (8)$$

where γ_{lv0} is the liquid-vapor interfacial tension at time zero with zero applied voltage, θ_0 is the initial contact angle, and $\theta(V,t)$ is the actuated contact angle. It should be emphasized here that adsorption and applied voltage are two main reasons for the change in the contact angle of the microdroplet. Finally, by using equations (5) and (7) equation (8) can be written as

$$\cos\theta(V,t)\left\{\gamma_{lv0}-\alpha_{lv}-\beta_{lv}+\left[\alpha_{lv}\exp\left(-\sqrt{\frac{4t}{\pi\tau_{lv}}}\right)+\beta_{lv}\right]\exp(-k_{lv}t)\right\}= \\ \frac{c(t)V^2}{2}+\alpha_{sl}+\beta_{sl}-\left[\alpha_{sl}\exp\left(-\sqrt{\frac{4t}{\pi\tau_{sl}}}\right)+\beta_{sl}\right]\exp(-k_{sl}t)+\gamma_{lv0}\cos\theta_0 \quad (9)$$

Equation (9) can be used to characterize the time-dependent behavior of the microdroplet and its interface in digital microfluidic systems. In the following sections, first, the experimental setup is introduced and the results obtained from equation (9) are verified by comparing the results with the experimental data. Finally, the proposed model is used to model the interaction of the microdroplet and system for different molecules.

3 RESULTS AND DISCUSSION

In this section, to verify the model, the results of the proposed model are compared to the experimental results, and the verified model is used to predict time-dependent behavior of the microdroplet and system due to the biomolecular adsorption to the interfaces.

3.1 Verification

Real-time characterization of the microdroplet and system is shown elsewhere [11]. It is shown here that by adding two new submodules (contact angle and capacitance sampling submodules) to the digital microfluidic implementations, properties of the microdroplet and system can be determined during the microdroplet transport. The schematic of the experimental submodules implemented in the digital microfluidic system is shown in Figure 1.

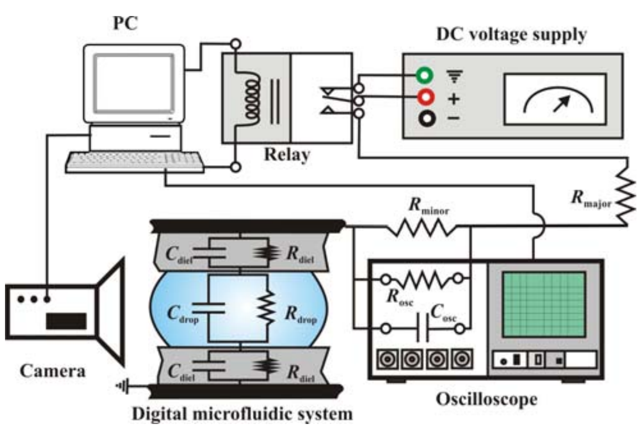

Figure 1: The schematic of the experimental submodules implemented in the digital microfluidic system [11].

The digital microfluidic system is comprised of two separated glass plates with 45 nm thick copper electrodes. The electrode pitch is 500 μm, the distance between two electrodes is 100 μm, and gap spacing is 250 μm. The electrodes are coated with a 200 nm PDMS layer providing both dielectricity and hydrophobicity. The fluids of interest, i.e., Bovine Serum Albumin (BSA, SIGMA A7906) aqueous solutions, are positioned between these PDMS coated electrodes. The electrodes are activated by a high voltage DC power supply (Stanford Research System, PS350) that is triggered by a relay (SANYOU, DSY2Y-S-205L) and a computer. The contact angle values of the microdroplet is determined simultaneously by means of digital imaging using a microscope (Leica Z6 APO) which is connected to a high resolution digital CCD camera. All experiments presented in this work were repeated three times for reproducibility and experimental validation.

In this subsection, to verify the proposed model, the calculated capacitance from equation (9) is compared to the measured capacitance of the system. This comparison is shown in Figure 2. As can be seen here, the capacitance values obtained from the model exhibit an error of only 3%.

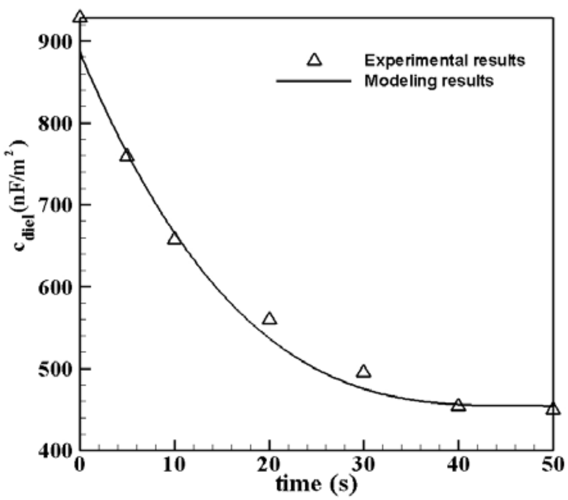

Figure 2: Calculated capacitance from equation (9) is compared to the measured capacitance [11] of the system.

3.2 Modeling

In this subsection, the proposed model is used to characterize the digital microfluidic system properties for two different solutions: BSA and lysozyme. Two main mechanisms have been identified for biomolecular adsorption in digital microfluidic systems [8]: passive adsorption which arises from the hydrophobic interactions and electrostatically driven adsorption due to applying an external voltage. It has been shown that the net charge of the molecules is one of the key parameters in defining the trend of the contact angle change over time [8]. These different trends can be observed in Figures 3 and 4 where the change in the contact angle is shown for three different molecules, i.e. pure water, BSA and lysozyme. The pH of all the solutions is 6.5. At this pH level, molecules of the BSA are negatively charged and molecules of the lysozyme are positively charged. Concentration of all the solutions is 4 μg/mL, and square wave potentials at a frequency of 0.1 Hz is applied (5 s at 0 V, 5 s at -30 V in Figure 3 and +30 V in Figure 4).

As it is shown in Figure 3, BSA and lysozyme, due to their different molecule charges, show different trends. When -30 V is applied, negatively charged BSA molecules are attracted to the positively charged surface; while positively charged lysozyme molecules are repelled. Thus, there is less surface adsorption, and the behavior of the lysozyme molecules is closer to that of water molecules.

As can be seen in Figure 4, the trend is reversed when the polarity is switched to +30 V. The behavior of BSA with -30 V is qualitatively similar to that of lysozyme with +30 V and vice versa.

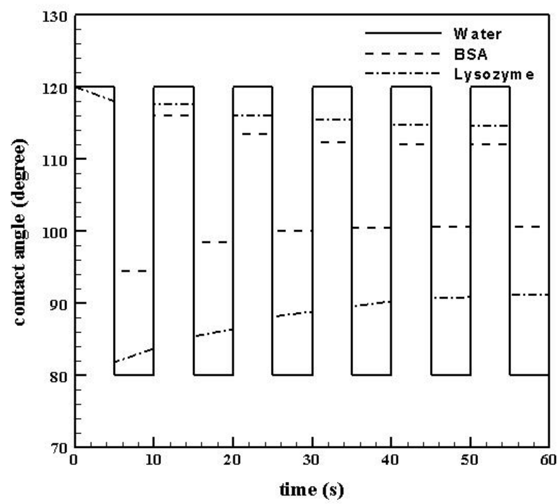

Figure 3: The change in the contact angle is shown for three different molecules, i.e. pure water, BSA and lysozyme. The pH of all the solutions is 6.5. Square wave potentials at a frequency of 0.1 Hz are applied (5 s at 0 V, 5 s at -30V).

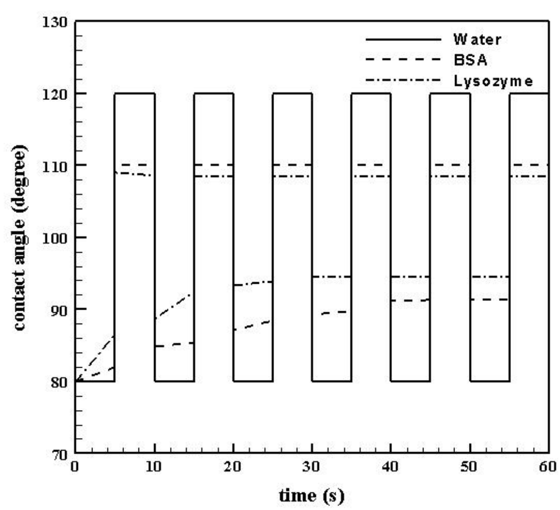

Figure 4: The change in the contact angle is shown for three different molecules, i.e. pure water, BSA and lysozyme. The pH of all the solutions is 6.5. Square wave potentials at a frequency of 0.1 Hz are applied (5 s at 0 V, 5 s at +30V).

The system characteristics can now be modeled by using equation (9). Capacitances of the system, for the negative and positive applied voltage over time, are shown in Figures 5 and 6. Results of Figures 3 and 4 are verified again here. BSA and lysozyme, due to their different charges, have different effects on the system (see Figure 5). When negative voltage is applied, the change in the capacitance of the system for BSA molecules is faster and more significant. However, Figure 6 shows a trend in which adsorption of the lysozyme molecules, and hence the change in the capacitance of the system, occurs faster.

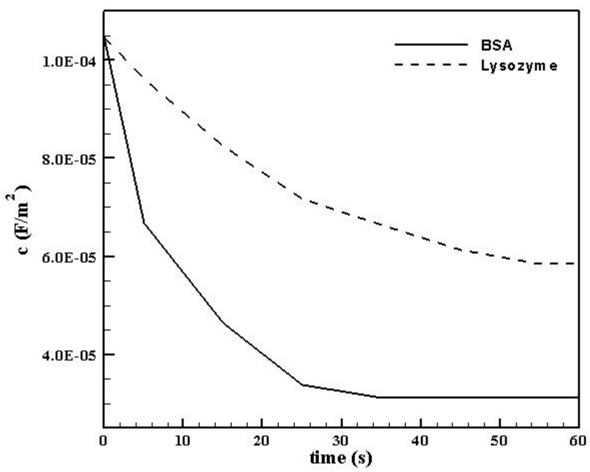

Figure 5: The change in the capacitance of the system is shown for two different molecules, i.e. BSA and lysozyme. The pH of all the solutions is 6.5. Square wave potentials at a frequency of 0.1 Hz are applied (5 s at 0 V, 5 s at -30 V).

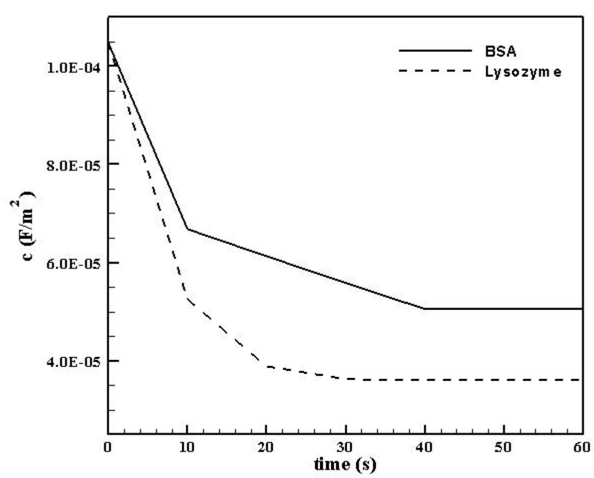

Figure 6: The change in the capacitance of the system is shown for two different molecules, i.e. BSA and lysozyme. The pH of all the solutions is 6.5. Square wave potentials at a frequency of 0.1 Hz are applied (5 s at 0 V, 5 s at +30 V).

4 CONCLUSION AND SUMMARY

In this paper, biomolecular adsorption in electrowetting-based digital microfluidic devices is modeled. The results obtained from the model are in excellent agreement with the experimental results. It is shown that the net charge of the molecules and polarity of the applied voltage are one of the key parameters in characterizing the adsorption phenomenon. It is found that by adjusting the polarity of the applied voltage according to the net charge of the molecules, effects of the nonspecific adsorption of these biomolecules can be reduced significantly.

REFERENCES

[1] M. G. Pollack, R. B. Fair and A. D. Shenderov, Appl. Phys. Lett. 77, 1725, 2000.

[2] J. Lee, H. Moon, J. Fowler, C. J. Kim and T. Schoellhammer, Proc. IEEE Int. Conf. MEMS, 499, 2001.

[3] M. Abdelgawad, A. R. Wheeler, Adv. Mater. 19, 133, 2007.

[4] R. B. Fair, A. Khlystov, T. D. Tailor, V. Ivanov, R. D. Evans, V. Srinivasan, V. K. Pamula, M. G. Pollack, P. B. Griffin and J. Zhou, IEEE Des. Test Comput. 10, 2007.

[5] R. B. Fair, Microfluid. Nanofluid. 3, 245, 2007.

[6] A. R. Wheeler, H. Moon, C. J. Kim, J. A. Loo and R. L. Garrell, Anal. Chem. 76, 4833, 2004.

[7] A. R. Wheeler, H. Moon, C. A. Bird, R. R. O. Loo, C. J. Kim, J. A. Loo and R. L. Garrell, Anal.Chem. 77, 534, 2005.

[8] J. Y. Yoon, R. L. Garrell, Anal. Chem. 75, 5097, 2003.

[9] F. Mugele, J. Baret, J. Phys. Condens. Matter 17, 705, 2005.

[10] W. van der Vegt, W. Norde, H. C. van der Mei and H. J. Busscher, J. Colloid Interface Sci. 179, 57, 1996.

[11] A. Ahmadi, K. D. Devlin, H. Najjaran, J. F. Holzman and M. Hoorfar, LOC, DOI: 10.1039/b925665b, 2010.